

Identifying and Forecasting Potential Biophysical Risk Areas within a Tropical Mangrove Ecosystem using Multi-Sensor Data

Shanti Shrestha^{a,f}, Isabel Miranda^{c,f}, Maria Luisa Escobar Pardo^{c,f}, Abhishek Kumar^{b,f}, Taufiq Rashid^{d,f}, Subash Dahal^{e,f}, Caren Remillard^{b,f}, Deepak R. Mishra^b

^a Warnell School of Forestry and Natural Resources, University of Georgia, Athens, GA 30602, USA

^b Department of Geography, University of Georgia, Athens, GA 30602, USA

^c Department of Geography, Clark University, Worcester, MA 01610, USA

^d College of Engineering, University of Georgia, Athens, GA 30602, USA

^e Department of Crop and Soil Sciences, University of Georgia, Athens, GA 30602, USA

^f NASA DEVELOP Program, University of Georgia, Athens, GA 30602, USA

Abstract

Mangroves are one of the most productive ecosystems known for provisioning of various ecosystem goods and services. They help in sequestering large amounts of carbon, protecting coastline against erosion, and reducing impacts of natural disasters such as hurricanes. Bhitarkanika Wildlife Sanctuary in Odisha harbors the second largest mangrove ecosystem in India. This study used Terra, Landsat and Sentinel-1 satellite data for spatio-temporal monitoring of mangrove forest within Bhitarkanika Wildlife Sanctuary between 2000 and 2016. Three biophysical parameters were used to assess mangrove ecosystem health: leaf chlorophyll (CHL), Leaf Area Index (LAI), and Gross Primary Productivity (GPP). A long-term analysis of meteorological data such as precipitation and temperature was performed to determine an association between these parameters and mangrove biophysical characteristics. The correlation between meteorological parameters and mangrove biophysical characteristics enabled forecasting of mangrove health and productivity for year 2050 by incorporating IPCC projected climate data. A historical analysis of land cover maps was also performed using Landsat 5 and 8 data to determine changes in mangrove area estimates in years 1995, 2004 and 2017. There was a decrease in dense mangrove extent with an increase in open mangroves and agricultural area. Despite conservation efforts, the current extent of dense mangrove is projected to decrease up to 10% by the year 2050. All three biophysical characteristics including GPP, LAI and CHL, are projected to experience a net decrease of 7.7%, 20.83% and 25.96% respectively by 2050 compared to the mean annual value in 2016. This study will help the Forest Department, Government of Odisha in managing and taking appropriate decisions for conserving and sustaining the remaining mangrove forest under the changing climate and developmental activities.

1. Introduction

Mangrove ecosystems are not only very productive but also have unique morphological, biological, and physiological characteristics that help them adapt to extreme environmental conditions including high salinity, high temperature, strong winds, high tides, high sedimentation, and anaerobic soils (Giri et al. 2011, Kuenzer et al. 2011). The halophytic

evergreen woody mangroves have a complex root system, salt-excreting leaves, and viviparous water-dispersed propagules (Kathiresan and Bingham 2001, Kuenzer et al. 2011). Mangroves provide numerous ecosystem services. For example, they can sequester large amounts of carbon compared to other forests (Das and Vincent 2009, Rodriguez et al. 2016) especially in the root systems and soil, estimated to be around 22.8 million metric tons of carbon each year, which is 11% of the total terrestrial carbon (Giri et al. 2011). They help in accumulation of sediments, contaminants and nutrients (Alongi 2002), thus acting as biological filters and maintain water quality. In addition, mangroves provide a buffer against erosion and storm damage, thus protecting coastal communities from adverse oceanic dynamics (Mazda et al. 1997, Blasco et al. 2001). They also serve as primary habitats and nurseries for birds, reptiles, insects, mammals, fish, crabs (Manson et al. 2005) and many marine flora, such as algae, seagrass, fungi etc. (Nagelkerken et al. 2008). They also provide food, timber, fuelwood, medicine to local population and cultural ecosystem services through the promotion of tourism and recreation.

Global mangroves constitute an area of 137,760 square km along tropical and subtropical climatic zones across 118 countries of the world (Giri et al. 2011). Naturally, global distribution of mangroves is governed by temperature but at regional scale, it is related to the distribution of rainfall, tides and waves that affect water circulation, which in turn affects the rate of erosion and deposition of sediments on which mangroves thrive (Alongi 2002). Southeast Asia possesses the largest proportion of global mangroves (Kuenzer et al. 2011) due to the favorable conditions. However, a recent study by Hamilton and Casey (2016) raised the issue of increased deforestation rates (3.58 % to 8.08%) in Southeast Asia. Natural disturbances like hurricanes, tsunami, storms, and lightning, also have been found to destroy millions of mangroves causing decline in mangrove extent in Southeast Asia. Furthermore, various studies have suggested numerous anthropogenic factors for declining habitats such as urban development, conversion to agricultural land (Reddy et al. 2007), aquaculture, mining, overexploitation for timber, fuelwood and fish, crustaceans and shellfish (Alongi 2002) and pollution (Giri et al. 2015). Recently, several studies have identified climate change as the largest global threat to mangrove in the coming decades (Blasco et al. 2001, Alongi 2002). It is predicted that climate change is going to intensively alter atmospheric and water temperature; timing, frequency and amount of rainfall; magnitude of sea-level rises; wind movements and frequency and severity of hurricanes (Solomon 2007). Though mangroves possess resistive capacity to withstand and recover from these changes; mangroves extent, composition and health may undergo changes when coupled with anthropogenic disturbances (Kandasamy 2017). Hence, an increasing need has been identified for global monitoring system of mangrove response to climate change (Field 1994). International programs, such as Ramsar Convention on Wetlands or the Kyoto Protocol have been advocating issues to prevent further loss of mangroves including regular monitoring of the ecosystem (Kuenzer et al. 2011). However, frequent monitoring is not possible with field data over a large spatial extent. This invokes the need for a rapid, frequent, and large-scale monitoring tool to help in conservation and restoration measures of mangroves. In this context, satellite based remote sensing has the potential to provide cost-effective, reliable and synoptic information to examine mangrove habitats and frequent monitoring over a large area. Particularly, in developing countries where geoinformation is rare, its use is immensely valuable.

Availability of open source historical and near real-time satellite data, increased range of image datasets at varying spatial, temporal and spectral resolutions (Kamal et al. 2015), areal

coverage from local to global scale, advances in low-cost sensor technologies and recent developments in the hardware and software used for processing a large volume of satellite data have helped increase the usefulness of remotely sensed data in environmental monitoring. Many scientific studies have been published regarding the potential of remote sensing to detect, map and monitor extent, species differentiation, carbon stock estimation, productivity and health assessment of mangroves throughout the world (Giri et al. 2011, Kamal and Phinn 2011, Bhar et al. 2013, Giri et al. 2015, Patil et al. 2015). Many studies have used moderate resolution satellite data to produce a long-term phenology and identify hotspots for early stages of mangrove degradation (Ibharim et al. 2015, Pastor-Guzman et al. 2015, Ishtiaque et al. 2016). A study by Ishtiaque et al. (2016) has shown the applicability of utilizing MODIS products to monitor biophysical health indicators of mangroves in order to analyze degradation in the Sundarbans. Guzman et al. (2015) assessed spatio-temporal variation in mangrove chlorophyll concentration using Landsat 8. Another recent study by Ibharim et al. (2015) used Landsat and RapidEye data to evaluate changes in land use/land cover and produced change detection maps of mangrove forests to determine threats toward these ecosystems. Recently, cloud computing such as Google Earth Engine (GEE) and Amazon Web Services (AWS) have provided unlimited capabilities for satellite data processing (Giri 2016). Chen et al. (2017) demonstrated the potential of using GEE platform to mangrove mapping for China. Studies have also shown the potential of synthetic aperture radar (SAR) data for mangrove mapping, especially to address the issue of data gap due to cloud coverage (Cougo et al. 2015, Kumar et al. 2017).

While many studies have assessed the status, and change of mangrove forests, very few studies have explored biophysical parameters of mangroves. While space and ground-based observations are useful in monitoring ecosystems, and assessing change-detection, they only consider past or current conditions or trends. Being able to assess an ecosystem in the future is important as it allows decision-makers to take precautionary steps and prepare for adverse future conditions (Nemani et al. 2007). Within the past decade climate forecasting capabilities of coupled ocean-atmosphere global circulation models (GCMs) have improved allowing for future climate trends to be applied on the ecosystem to forecast biophysical and land-cover conditions (Zebiak 2003, Nemani et al. 2007). Advent of tools like TerrSet Land Change Modeler have now allowed prediction of future land-cover transitions. Availability of data such as NASA's Giovanni derived meteorological parameters and WorldClim projected spatial data have provided avenues for predicting how mangrove ecosystems will change in the future in response to environmental factors.

This study aims at integrating data from multiple satellite sensors with projected meteorological variables to achieve forecasting of mangrove biophysical characteristics of Bhitarkanika Wildlife Sanctuary to predict future risk to mangrove extent as well as their ecological health status. Specific objectives of this study are to i) calibrate and validate the models to predict biophysical parameters (GPP and LAI) using surface reflectance data obtained from MODIS for 17 years (2000-2016), ii) analyze spatio-temporal variability in the biophysical parameters, iii) to forecast and map biophysical parameters at year 2050 using hydro-meteorological data, and iv) to perform land use-land cover (LULC) classification and forecast of mangrove land cover. To the best of our knowledge, this is a novel study in terms of ecological forecasting based on biophysical parameters using multi-sensor multi-source data. The study was carried out to investigate the land cover and biophysical characteristics of mangroves in Bhitarkanika Wildlife Sanctuary that harbors the second largest mangrove ecosystem of India. A

large population depends on these mangroves for livelihood including food, raw materials, medicinal and ornamental products (Hussain and Badola 2010). Mangroves in this region are dynamic and threatened because of many drivers including over-exploitation and conversion to agricultural land (Reddy et al. 2007), overfishing, firewood extraction, and climatic changes. Few studies have assessed vegetation composition, phenology and areal extent of mangroves in Bhitarkanika (Reddy et al. 2006, Upadhyay and Mishra 2010, Behera and Nayak 2013). However, information on the temporal behavior of mangrove forests and their biophysical parameters is limited. This study attempts to not only understand the dynamism but also predict how mangrove ecosystem of this region will change in future in response to climatic factors. This study would provide environmental managers with ecological data for informed national and international management of mangrove ecosystems.

2. Materials and Methods

2.1 Study Area

Bhitarkanika is the second largest mangrove ecosystem in India situated on the east coast of the country, between 20°33' – 20°47' N latitude and 86°48' - 86°03' E longitude. It lies in the estuarine region of Brahmani, Dhamra and Baitarani rivers in the northeastern corner of Kendrapara District in the state of Odisha. With an extensive area of 672 sq. km, the wetland was declared as Wildlife Sanctuary in 1975 and a core area of 145 sq. km has been declared as Bhitarkanika National Park in 1992. It falls under tropical monsoon climate with three distinct seasons- winter (October-January), summer (February-May) and rainy (June-September) and frequently experiences tropical cyclones. The wetland is a habitat for the large population of salt water crocodiles, turtles, many endangered mammals and avian population. Additionally, it supports an exceptional floral diversity with around 62 species of mangroves (Chauhan and Ramanathan 2008). Being a wetland with rich biodiversity, this mangrove habitat has been designated as a Ramsar site of international importance in year 2002. Figure 1 shows the location and areal extent of mangroves of Bhitarkanika Wildlife Sanctuary.

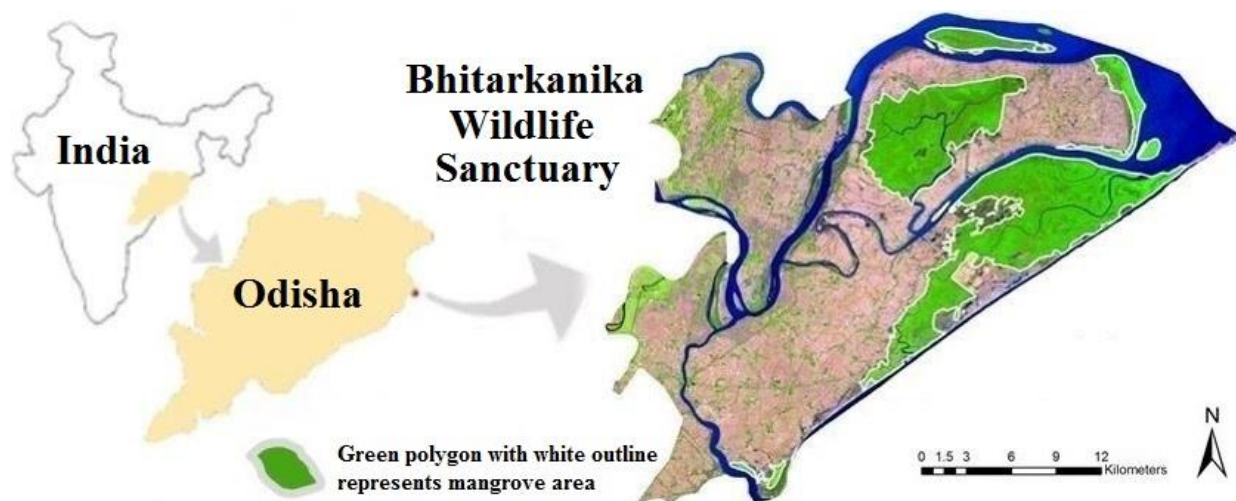


Fig. 1. Study area map corresponding to Bhitarkanika Wildlife Sanctuary showing mangrove area in green color. Landsat 8-OLI band combinations [R (6): G (5): B (2)] were used to create the map.

2.2 Data Acquisition

Satellite data from multiple sensors were acquired from April 1995 to May 2017 (Table 1). Cloud-free Landsat 5 Thematic Mapper (TM) and Landsat 8 Operational Land Imager (OLI), surface reflectance (r) products were downloaded from the United States Geological Survey (USGS) EarthExplorer website corresponding to Bhitarkanika Wildlife Sanctuary for Land Use Land Cover (LULC) classification. Sentinel-1 products were downloaded from the European Space Agency (ESA) Scientific Data Hub website to achieve high spatial resolution (10m) and improve the accuracy of LULC classification. Terra MODIS 500 m Level-2G 8-day average products including surface reflectance (MOD09A1), LAI (MOD15A2H) and GPP (MOD17A2H) products were downloaded from NASA's Level 1 and Atmosphere Archive and Distribution System (LAADS) website for biophysical (LAI and GPP) model calibration and long-term (2000-2016) seasonal and annual trend analysis.

Table 1

Data Acquisition Chart. Cloud-free satellite images were downloaded from April 1995 to May 2017.

Satellite	Sensor	Product	Temporal Resolution	Spatial Resolution (m)	Source
Landsat 5	Thematic Mapper (TM)	Surface Reflectance (r)	16-day	30	USGS Earth Explorer
Landsat 8	Operational Land Imager (OLI)	Surface Reflectance (r)	16-day	30	USGS Earth Explorer
Sentinel-1	Synthetic Aperture Radar (SAR)	High Resolution Ground Range Detected (GRD) Level-1 (IW mode)	12-day	10	ESA Scientific Data Hub
Terra	Moderate Resolution Imaging Spectroradiometer (MODIS)	Level-2G Surface Reflectance (MOD09GQ)	1-day	250	NASA's Level 1 and Atmosphere Archive and Distribution System (LAADS)
		Level-2G Surface Reflectance (MOD09A1)	8-day	500	
		Leaf Area Index (LAI)	8-day	500	

		(MOD15A2H)			
		Gross Primary Productivity (GPP) (MOD17A2H)	8-day	500	

Furthermore, to achieve forecasting objective, we incorporated physical-meteorological parameters corresponding to Bhitarkanika Wildlife Sanctuary and its watershed. Area averaged time series (January 2000-December 2016) data were downloaded from the NASA's Giovanni web-based application interface. These data included monthly averaged precipitation from Tropical Rainfall Measuring Mission (TRMM) products, monthly averaged surface runoff, and surface temperature (Table 2). Kumar et al. (2017) incorporated similar physical-meteorological parameters to isolate the impact of these variables on Bhitarkanika mangrove's biophysical parameters. All data were first visualized using the NASA Giovanni web interface and corresponding ASCII files were downloaded for each parameter for further analysis. The projected (2050) precipitation and temperature data were acquired from the WorldClim website (<http://www.worldclim.org/>).

Table 2
Physical-meteorological variables used in this study.

Physical-Meteorological Variables	Product Name	Source
Precipitation	TRMM_3B43_v7	NASA Giovanni
Surface Runoff	GLDAS_NOAH025_Mv2.1	NASA Giovanni
Surface Temperature	GLDAS_NOAH025_Mv2.1	NASA Giovanni
Projected Temperature (2050)	GISS-E2-R (RCP 4.5)	WorldClim
Projected Precipitation (2050)	GISS-E2-R (RCP 4.5)	WorldClim

2.3 Data Processing and Analysis

Data processing and analysis were accomplished in two parallel components to achieve the objectives of this study. The first component included land cover classification for change detection and forecasting the threatened mangrove areas within the study site. The second component included re-parameterizing existing mangrove biophysical models (LAI and GPP) and establishing a relationship between biophysical and meteorological parameters to achieve forecasting objective. Finally, a qualitative comparison between forecasted land cover risk map and forecasted biophysical parameters maps was carried out to observe the spatial similarity between both. The detailed description of each component is presented in following sub-sections.

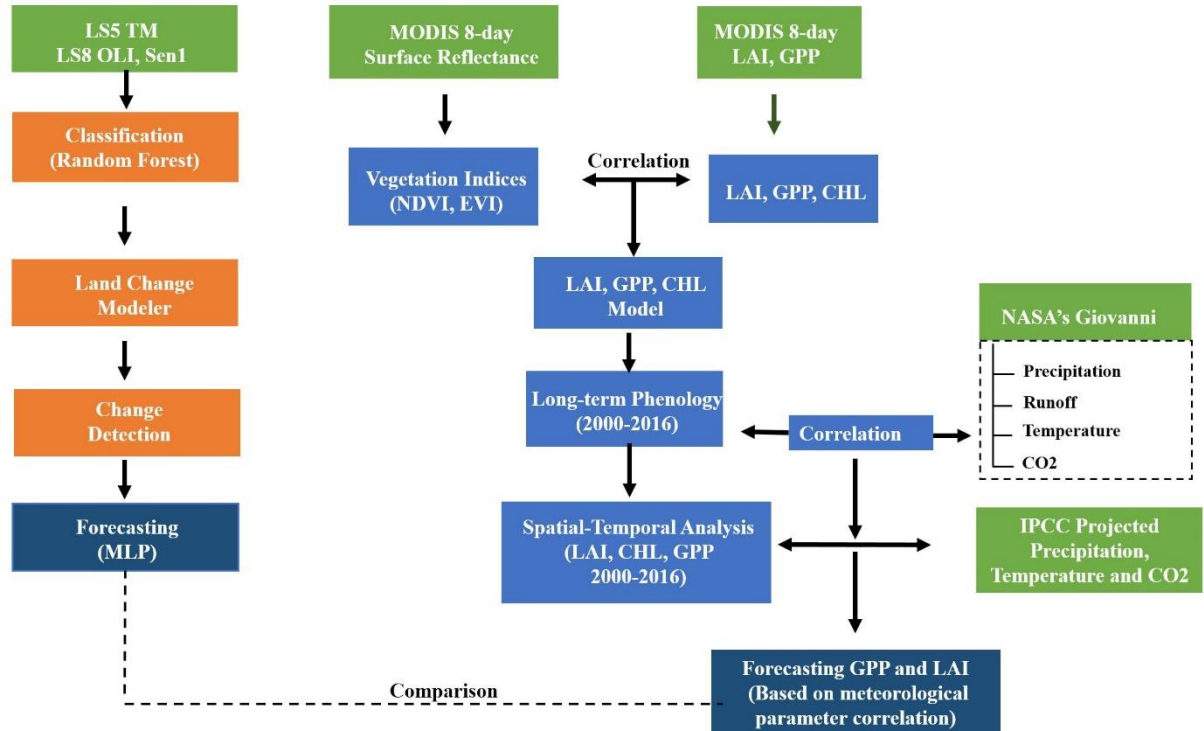


Fig. 2. Overall methodology and various remote sensing datasets utilized in forecasting mangrove biophysical parameters and future risk assessment.

2.3.1 Land Cover Classification and Validation

LULC classification was carried out for 22 years (1995-2017) using Landsat 5 TM, Landsat 8 OLI, and Sentinel-1 data. To accomplish land use/land cover classification, training site polygons were created for seven land cover classes: dense mangrove, open mangrove, water, agriculture, mudflat, sand and plantation. The false-color composites (Landsat 5 and Landsat 8) and Google Earth Imageries were used as reference to distinguish land cover classes. The classification map of Pattnaik et al. (2008) was used as reference for validating Landsat 5 TM derived LULC map result of 2004. The 1995 and 2017 classifications were cross-referenced with their respective false-color composites and Google Earth Imagery. GEE Explorer was used to create a supervised classification and the random forests algorithm was used to classify the imagery. Random Forests is a machine learning technique that is being increasingly used for image classification of percentage tree cover and forest biomass (Horning 2010) and this algorithm is good for dealing with outliers in training data. It calculates classification error using one third of the training data (out-of-the-bag samples) while the remaining two thirds of the data is used to build the Random Forests Model (Horning 2010). Moreover, random forests provide fast and higher accuracy compared to other well-known classifiers for remotely sensed data (Gislason et al. 2006).

Output land cover maps were validated visually with stratified sample points using Google Earth satellite imagery at the closest timestamp. In addition, published literatures were referenced to maximize the accuracy of the land cover classification (Reddy et al. 2007, Pattanaik et al. 2008). An accuracy assessment was performed in TerrSet Geospatial Monitoring and Modeling Software (Clark Lab, Worcester, MA) to create an error matrix indicating the

producer's and user's accuracy. Additionally, the random forests algorithm produces an accuracy assessment using out-of-bag samples which was used to compare with the error matrix accuracy assessment. Finally, the classified maps were used to calculate the total area in square kilometers for each land cover class.

2.3.2 Mangrove Forest Cover Change Analysis

The LULC classification result was incorporated for change detection in TerrSet Land Change Modeler (LCM). The Land Change Modeler suite (LCM) in TerrSet was run to quantify land cover category change in the study area from 1995 to 2004 and from 2004 to 2017. The LCM output consists of land cover gains, losses, and persistence of each period as well as graphs of the contributors to change experienced by each land cover category. Several studies have used the LCM to map land cover change and predict future land-cover transitions based on user-specific drivers of change (Rodríguez Eraso et al. 2013, Weber et al. 2014).

To predict future land cover transitions, the transition potential and change allocation tab in the LCM were used. Land cover transitions that had less than 1,500 pixels of transition to another land cover class were excluded from the transition potential modeling. Therefore, only three transitions were used to run the transition sub model: dense mangrove to open mangrove, open mangrove to agriculture, dense mangrove to agriculture. Each transition has its own sub-model with a set of driver variables that will influence transitions of dense and open mangrove classes to another land cover class. These driver variables consist of temperature, precipitation, distance from roads, distance from channels and distance from disturbance (open mangrove to agriculture).

2.3.3 Forecasted Risk Map Analysis

To predict future changes in land cover, it was necessary to empirically model each of the transitions; this was done using the Multilayered Perceptron (MLP) Neural Network. The MLP was chosen because it can handle multiple transitions at once and because the driving forces for these transitions are the same. The MLP Neural Network selects a random sample of pixels that might have or have not transitioned in each of the land cover transitions (e.g., dense mangrove to open mangrove) that the user incorporated in modeling (Eastman 2015). Half of the sample pixels were used to train the model and the other half were used to test how well the model performed at predicting change. The MLP creates a multivariate function that can predict the potential for a pixel to transition based on the values of the driver variables for that pixel (Eastman 2015). The model produces an accuracy of how well the driver variables can predict change. The MLP produces a transition potential image that describes the probability that a transition will occur in the landscape and is used to predict future land cover change. The change demand modeling panel was used to predict future transition of land cover change for the year 2050. A soft prediction map which indicates a scale of vulnerability was used to show the risk of mangroves in the future. A soft prediction model is a “comprehensive assessment of change potential and also yields to a map of vulnerability to change that habitat and biodiversity assessments prefer” (Rodríguez Eraso et al. 2013, Eastman 2015).

2.3.4 Biophysical Models Re-parameterization

A recent study on Bhitarkanika mangroves by Kumar et al. (2017) utilized vegetation indices including Enhanced Vegetation Index (EVI) and NDVI (Eqs. 1-2) based biophysical

models (Eqs. 3, 4, & 5) to estimate mangroves LAI, GPP, and CHL. Because of the same study site, the relationship established between vegetation indices and biophysical parameters by Kumar et al. (2017) (Eqs. 3-5) were used as base models for re-parameterization in this study. When compared with standard MODIS LAI and GPP values extracted from MOD15 and MOD17 products, Kumar et al. (2017) models-derived LAI and GPP showed over prediction and hence, these two models were re-parametrized using 17 years of MODIS surface reflectance (ρ), MODIS LAI (MOD15), and MODIS GPP (MOD17) products from 2000-2016. However, re-parameterization was not carried out for CHL model (Eq. 5) due to lack of a standard MODIS based CHL product for terrestrial sites.

$$EVI = \frac{2.5 * [\rho(NIR) - \rho(Red)]}{[(1 + \rho(NIR) + 2.4 * \rho(Red))]} \quad (1)$$

$$NDVI = \frac{[\rho(NIR) - \rho(Red)]}{[\rho(NIR) + \rho(Red)]} \quad (2)$$

$$LAI = 17.155 * EVI^2 - 2.5745 \quad (3)$$

$$GPP = 0.0983 * EVI^2 + 0.0161 \quad (4)$$

$$CHL = 127 * NDVI - 46.61 \quad (5)$$

To re-parametrize biophysical models, 17 years (2000-2016) of ρ , LAI, and GPP data from MODIS 8-day products were extracted. A fish-net with spatial resolution of 500 m by 500 m was created across Bhitarkanika Wildlife Sanctuary (Figure 3) for extracting long-term data. Data extraction for mangrove pixels was performed using batch processing methods in European Space Agency (ESA)'s Sentinel Application Platform (SNAP) software and Esri's ArcGIS. A total of 130 pixels (n=130) were selected (red circles inside fish net in Figure 3) for data extraction after excluding non-mangrove and mixed pixels within the study area. The EVI values corresponding to these 130 pixels were regressed over long-term (2000-2016) GPP and LAI values derived from standard MODIS products- MOD17A2H and MOD15A2H respectively from same pixel locations to get regression coefficients to predict GPP and LAI. To confirm the validity of re-parametrized models, MODIS data was randomly separated into two sets for calibration (12 years) and validation (5 years) and models were fit to the two datasets separately. GPP and LAI values estimated from re-parameterized model were then compared with MODIS-product derived values to calculate root mean square error (RMSE) and percentage normalized root mean square error (%NRMSE).

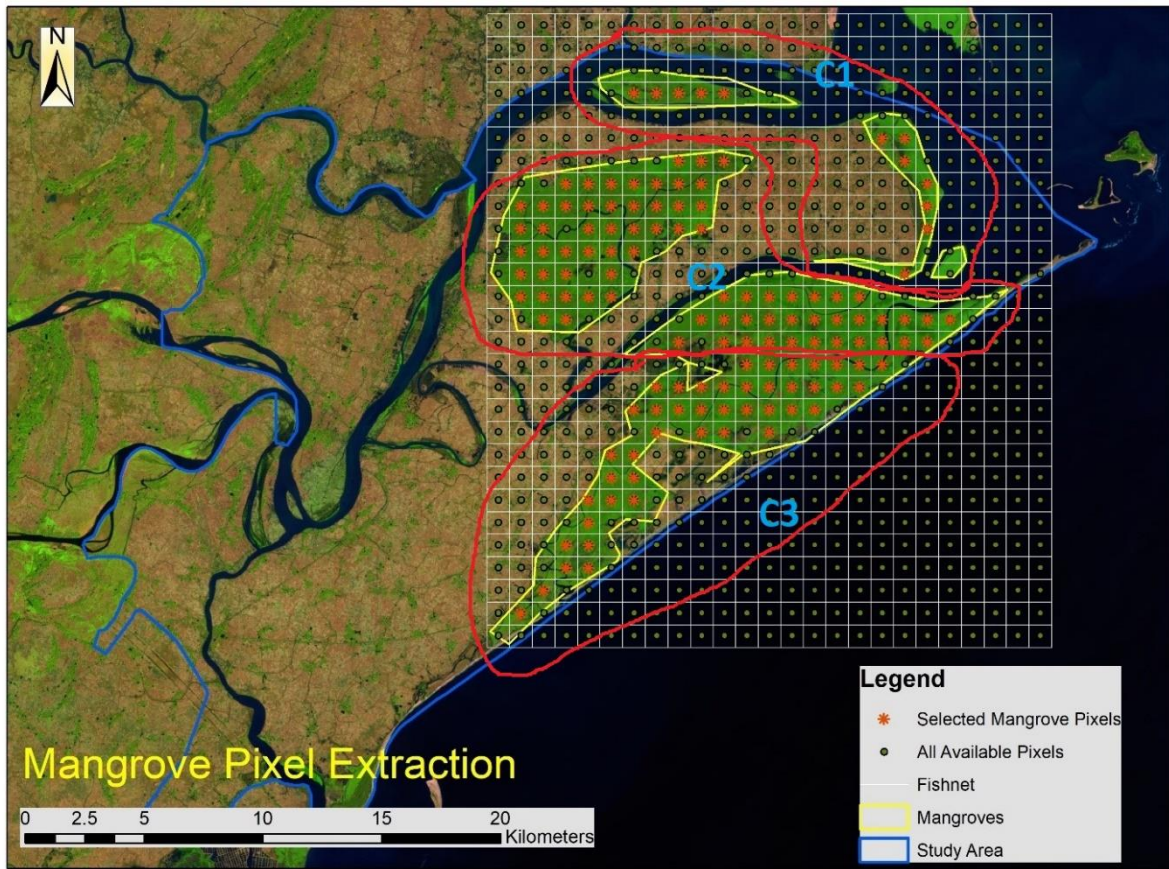


Fig. 3. Selected point locations for extraction of the pure Mangrove pixels (Total 130 pixels). A fish net of 500m x 500m area was created to extract data from 500m MODIS pixels. C1, C2 and C3 represent isolated cluster, dense cluster and open cluster respectively.

2.3.5 Long-term Spatio-temporal Variability

MODIS 8-day products derived LAI, GPP, and CHL data were analyzed monthly and annually in Microsoft Excel and R. LAI, GPP, and CHL data were averaged monthly for each year (2000-2016) for seasonal and inter-annual analysis. In order to analyze spatial variability, study area was sub-divided into three clusters as per spatial location of mangrove pixels such that the clusters were homogeneous within and heterogeneous among clusters. C1 denotes isolated clusters of mangroves, C2 denotes dense patches of mangroves and C3 denotes open mangroves (Figure 3).

2.3.6 Relationship between Biophysical Parameters and Climatic Variables

NASA's Giovanni derived physical and meteorological data were processed in Microsoft Excel and R (R Develop Core Team, 2015) for regression analysis with long-term LAI, CHL, and GPP. Physical-meteorological long-term data (2000-2016) were averaged monthly for correlating with biophysical parameters. Data from monsoon season (June, July, August, September) were not included in correlation analysis between biophysical parameters (LAI, GPP, and CHL) and physical-meteorological variables because of lack of cloud free-quality data

for those months. Apart from direct correlation between mangrove biophysical characteristics and physical-meteorological parameters, a time-lag analysis was also carried out during single and multivariate correlation analysis.

2.3.7 Forecasting Biophysical parameters

Projected (2050) climate data including precipitation and temperature were downloaded in GeoTiff format and imported in ArcMap software where they were extracted using a mask of the study area. They were then resampled to match with MODIS resolution (500m x 500m) and climatic data were extracted at mangrove pixel locations (130 pixels) within the study area. Based on the long-term (2000-2016) regression coefficients derived from relationship between each of the biophysical parameters, and meteorological parameters (temperature and precipitation), we estimated monthly LAI, GPP, and CHL for 2050 (using monthly forecasted precipitation and temperature) corresponding to all 130 mangrove pixels within the study area. These monthly LAI, GPP, and CHL from 130 pixels were averaged for 12 months to estimate annual averaged value for each biophysical parameter. Further, to create annual spatial maps, those 130-pixel averaged values corresponding to LAI, GPP, and CHL were imported in ArcMap and interpolation was carried out using IDW (Inverse Distance Weighted) tool to produce 2050 forecasted mangrove biophysical parameters spatial maps. There are other factors that could affect mangrove ecosystem that the study did not take into consideration such as sea-level rise, atmospheric carbon-dioxide level, salinity level, natural and anthropogenic disturbance. The forecasting method assumes that all other natural and anthropogenic factors remained unchanged.

3. Results & Discussion

3.1 Land cover Analysis

3.1.1 Land Cover Classification

Land cover classification was performed to study mangrove extent and to monitor changes over time. The classified land cover maps are shown in Figure 4. These classification results have an overall accuracy of 84% for 1995, 82% for 2004 and 86% for 2017. As can be seen in Figure 4, mangrove extent changed constantly over the study period. Mangroves have been considered a highly dynamic ecosystem by many studies (Giri et al. 2015, Rodriguez et al. 2016) due to simultaneous processes of erosion and accretion happening in the area (Giri et al. 2015) and complex interactions between mangroves habitat and environmental factors (Rodriguez et al. 2016). Areas with open mangrove in 1995 were replaced by dense mangrove in 2004. The subsequent increase in mangrove cover can be attributed to intensive plantation and conservation efforts. As compared to the classified image of 1995, one can see that the mangrove extent has increased in the proximity of water in 2004. Changes from water to mangroves have been attributed to sedimentation and formation of new grounds for mangrove establishment (Giri et al. 2007, Reddy et al. 2007, Ward et al. 2016). There was also decrease in mudflat areas in 2004 along the southern coastal strip. Reddy et al. (2007) also found that mudflat areas have reduced from 1973 to 2004 in Bhitarkanika due to increase in plantation area. Deforested or degraded patches of dense mangrove were identified in 2017 that were lost to open mangrove,

owing to different anthropogenic and natural drivers. RADAR data were used for 2017 land use classification. Radar data derived classification also showed a similar pattern of conversion of dense mangroves to open mangroves and classification of radar data showed highest accuracy (86.8%) compared to Landsat image classification. Radar data have high spatial resolution compared to many other hyperspectral optical sensors and a temporal resolution of 12 days. Radar data have comparable results with optical sensors and particularly useful for capturing rainy season data, when data are limited due to cloud cover (Kumar et al. 2017). In view of benefits of radar data, they have been applied to vegetation/land cover mapping and monitoring (Held et al. 2003, Joshi et al. 2016) and have the potential to be used for classification in future research.

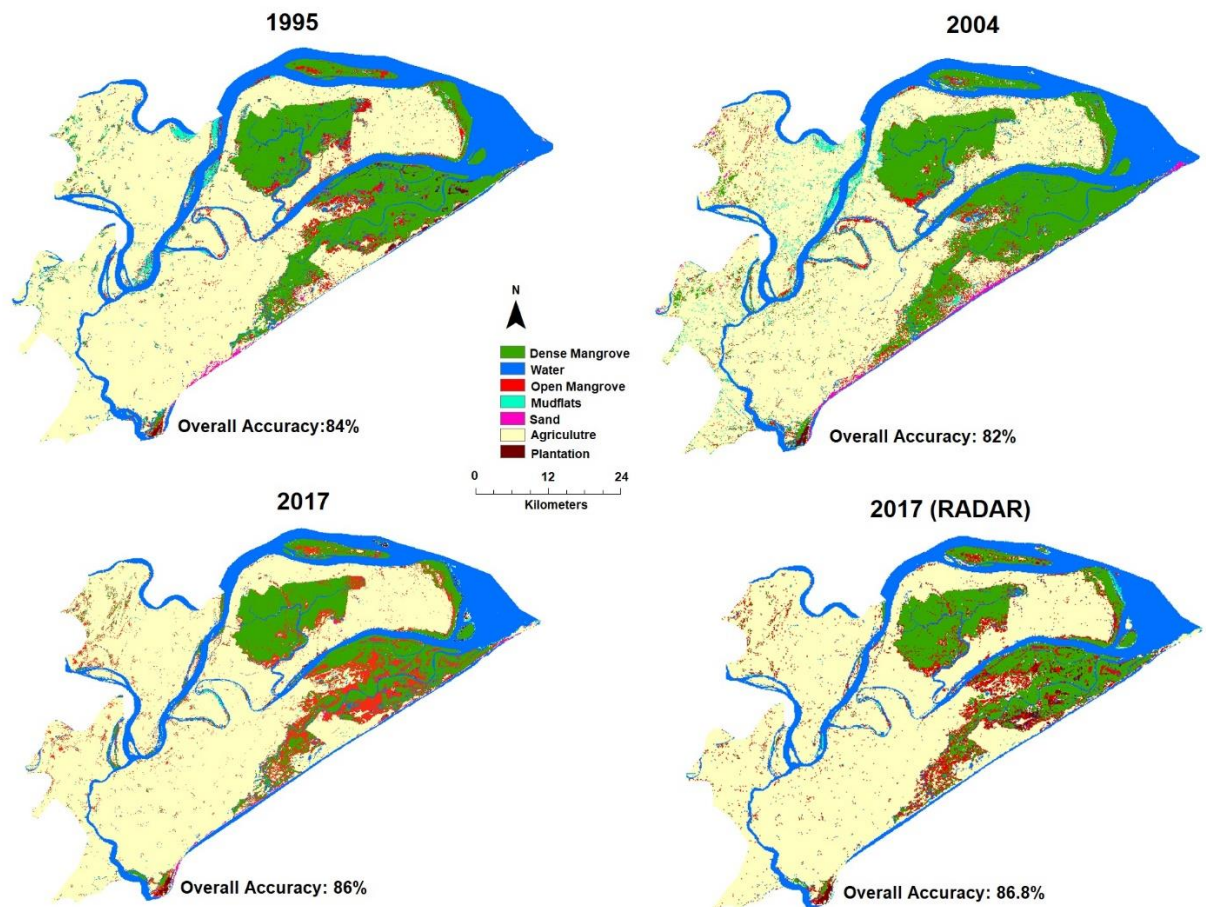


Fig. 4. Land cover classification using Landsat 5-TM (1995, 2004), Landsat 8-OLI (2017), and Sentinel 1 (C-SAR) Radar data (2017).

3.1.2 Mangrove Forest Cover Change Analysis

Land Change Modeler in TerrSet was used to map areas of gain, loss and persistence of dense mangroves in Bhitarkanika. The total amount of loss of dense mangrove was 9.28 square km from 1995 to 2004 and the total amount of loss from 2004 to 2017 was 21.44 square km, indicating more loss occurred between 2004 and 2017 than between 1995 and 2004. Zooming into a part of the study area (shown bounded by blue box in Figure 5), it was observed that in

1995, areas of open mangroves were replaced by dense mangroves in 2004. The government of Odisha had declared core area of Bhitarkanika as a National park in 1998. The resultant gain of 24.4% of dense mangrove could be attributed to increased protection and consequent regeneration. On the other hand, 70% of the total dense mangroves again changed into open mangroves from 2004 to 2017 in the area. Conversion of dense to open mangroves is an indication of forest degradation, likely due to encroachment and over-exploitation for resources resulting from lack of strict law enforcement. Literature suggest that the major causes of mangrove forest loss include conversion to agriculture, urban development, shrimp farming, over harvesting, pollution, siltation and natural disturbances like reduction in freshwater flow etc. (Giri et al. 2015).

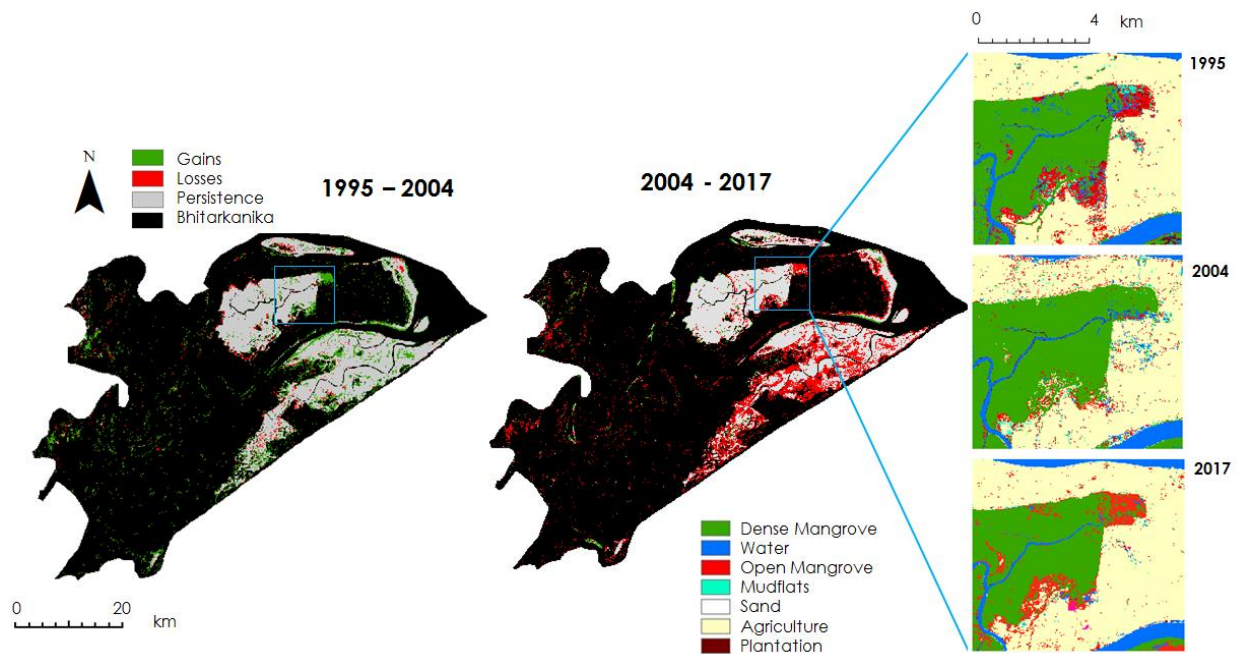


Fig. 5. Dense mangrove changes from 1995 to 2004 and 2004 to 2017

3.1.3 Forecasted Risk Map Analysis

Based on the patterns of decadal changes, LULC changes were predicted for year 2050 to analyze risk of mangrove to disturbance in future. The MLP produced a soft prediction map that indicated a scale of mangrove risk to disturbance in 2050. Red to orange locations indicated medium to high vulnerability and locations of yellow to blue indicated lower vulnerability (Figure 6). In the northern part of Bhitarkanika, lower mangrove risk locations were demarcated in blue while the edges of the mangrove extent indicated higher mangrove risk to disturbance in red. The medium to high mangrove risk to disturbance (in yellow and red) was in the southern part of the study area, below the Rajnagar-Pattamundai road and along the river. Another model that the Markov Chain analysis in MLP outputs was the hard prediction, which was a “best guess” of the many plausible scenarios that land cover could have in the future. The chances that the hard prediction would match future conditions are slim and should be interpreted with caution. The soft prediction model provided a better indication about risks to habitat and biodiversity. The hard prediction map compared to the 2017 classification map showed a greater

increase in agriculture from open mangrove. The soft prediction map also located areas of high mangrove risk that coincided with open mangrove areas in the 2017 classification map.

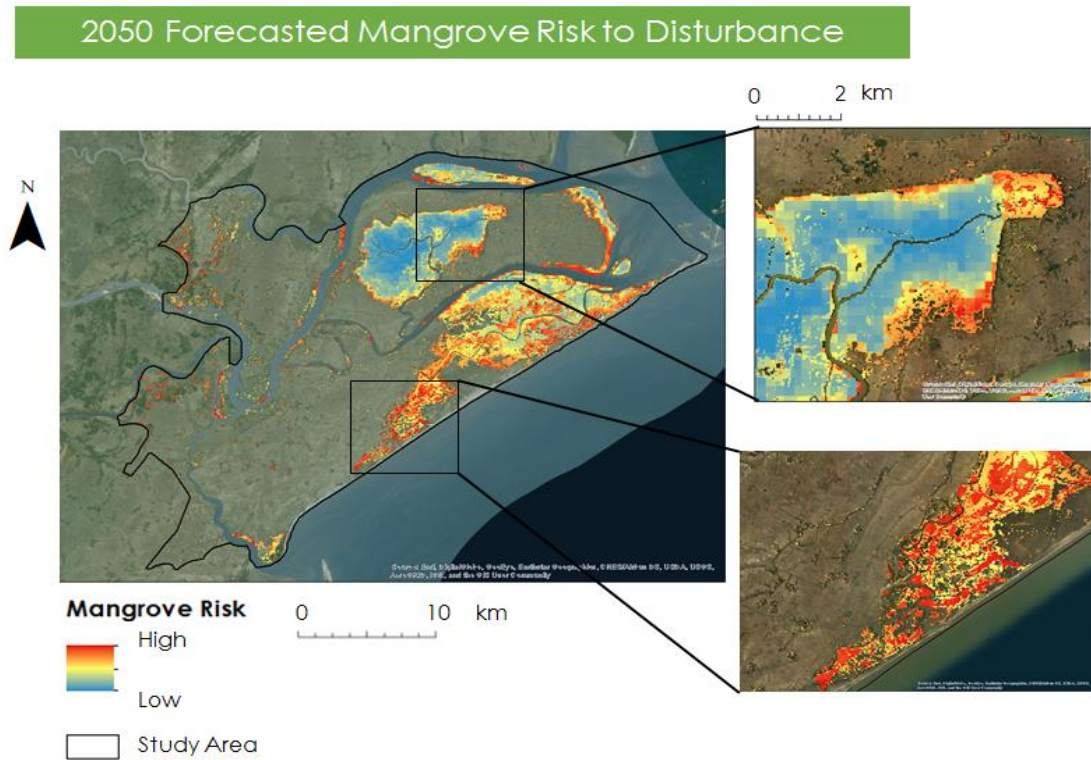


Fig. 6. The soft prediction map for 2050 mangrove extent indicated the scale of risk of mangroves to disturbance. Red indicates high mangrove risk and blue indicates low mangrove risk.

3.2 Biophysical Parameter Analysis

3.2.1 Biophysical Model Re-parameterization

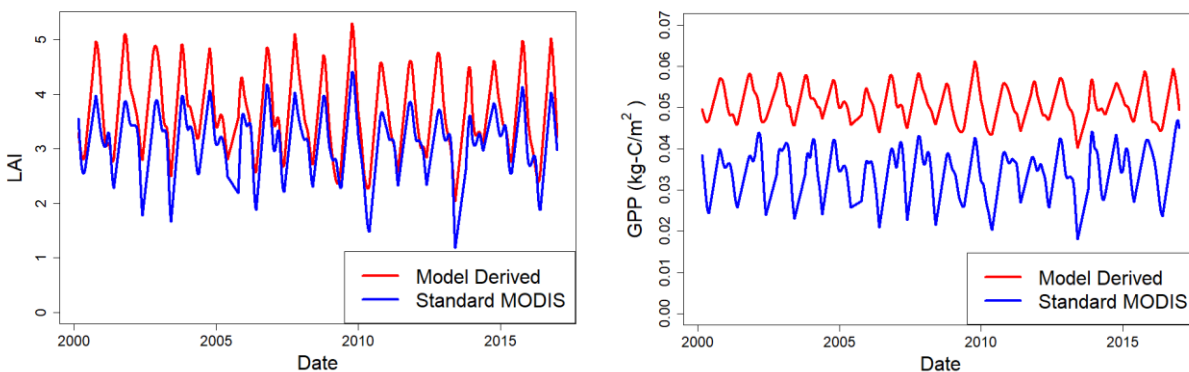


Fig. 7. Comparison between MODIS standard LAI and GPP and model derived LAI, GPP.

Figure 7 shown above compares the time-series of LAI and GPP derived from models developed by Kumar et al. (2017) and standard MODIS products. The model-derived LAI and GPP showed over prediction. This is mainly because Kumar et al. (2017) LAI and GPP models were developed using only 20 selective pixels randomly distributed over study area that belonged to mostly dense mangrove patches from only few years of data, which produced systematic bias towards higher values. Therefore, these models were reparametrized using 17 years (2000-2016) of data. The re-parameterized models corresponding to LAI and GPP are presented below in Equations 6 and 7 respectively.

$$\text{LAI} = 11.80 \cdot \text{EVI} - 1.041 \quad (6)$$

$$\text{GPP} = 0.096 \cdot \text{EVI} + 0.0003 \quad (7)$$

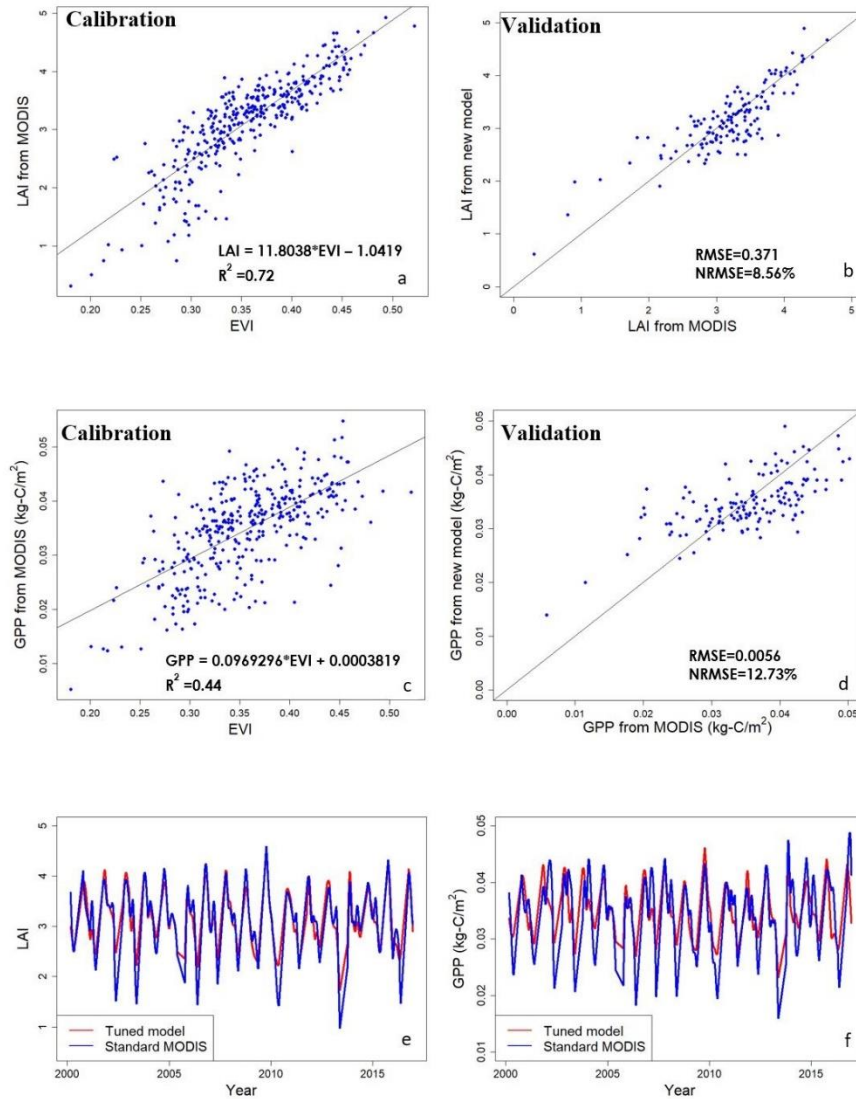


Fig. 8. Re-parameterized LAI model calibration and validation (a-b). Re-parameterized GPP model calibration and validation (c-d). Comparison between MODIS standard LAI, GPP and re-parameterized model derived LAI, GPP (e-f), that also showed inter-annual variability of the parameters.

The calibration and validation results showed improvement in the re-parameterized models with reduced NRMSE of 8.56% for LAI model and 12.73% for GPP model, compared to earlier models' NRMSE which was 19.54% for LAI and 18.64% for GPP. The time series of GPP and LAI from re-parameterized model clearly resolved the systematic overestimation issue in prediction (Figures 8: e-f), which was encountered before (Figure 7).

3.2.2 Long-term Spatio-temporal Variability

To identify the effects of climate change and different disturbances on mangrove requires long term monitoring of biophysical parameters. Analysis of the long-term biophysical parameters showed trends and seasonality (Figure 9). Temporal analysis revealed a phenological pattern which peaks during September and October, corresponding with the fall season, and dips during summer months of April and May. This seasonal pattern is consistent with previous study by Kumar et al. (2017). Seasonal variability of the biophysical parameters can be attributed to variability in soil moisture and salinity levels (Kumar et al. 2017). During fall season, temperature is relatively less, and land surface usually is replenished with water thus resulting in reduced salinity and hence more greenery. During dry summer months, salinity levels remain high reducing light use efficiency and hence photosynthesis in leaves (Parida et al. 2002), impairing productivity. Decrease in the LAI indicates a decrease in canopy foliage and decrease in GPP indicates decrease in productivity.

The spatial distribution of biophysical characteristics in Bhitarkanika showed dynamic changes as well. The study area was sub-divided into three clusters as per spatial location of mangrove pixels to analyze spatial variability. The cluster-wise analysis of mangrove pixels suggested that cluster 2 (C2) which was dominated by dense mangrove, showed highest values for all biophysical parameters (mean GPP: 0.037 kg-C/m²; mean LAI: 3.38; mean CHL: 39.43 g-C/m²). This is because they have closed canopy and are mostly composed of diverse species adapted to thrive on tidal swamps (Reddy et al. 2007). In contrast, isolated clusters (C1) had relatively lowest values of GPP (mean: 0.032 kg-C/m²), LAI (mean: 2.8), and CHL (mean: 29.37 µg/cm²) (Table 3). Also, cluster 3 (C3), which was dominated by open mangroves, showed lower mean value for all parameters-GPP (mean: 0.033 kg-C/m²), LAI (mean: 2.91), and CHL (mean: 33.17 µg/cm²).

Table 3:

Cluster-wise variability in MODIS derived GPP, LAI, and CHL for 17 years (2000-2016) of data analyzed for Bhitarkanika Wildlife Sanctuary.

Parameter statistics	Isolated	Dense	Open
GPP (kg-C/m²)			
Min	0.005	0.010	0.009
Max	0.046	0.053	0.050
Mean	0.032	0.037	0.033
SD	0.006	0.006	0.005
LAI			
Min	0.36	0.83	1.19

Max	4.5	5.35	4.95
Mean	2.8	3.38	2.91
SD	0.74	0.43	0.63
CHL ($\mu\text{g}/\text{cm}^2$)			
Min	3.22	7.1	4.45
Max	54.55	58.79	54.3
Mean	29.37	39.43	33.17
SD	11.29	10.75	10.06

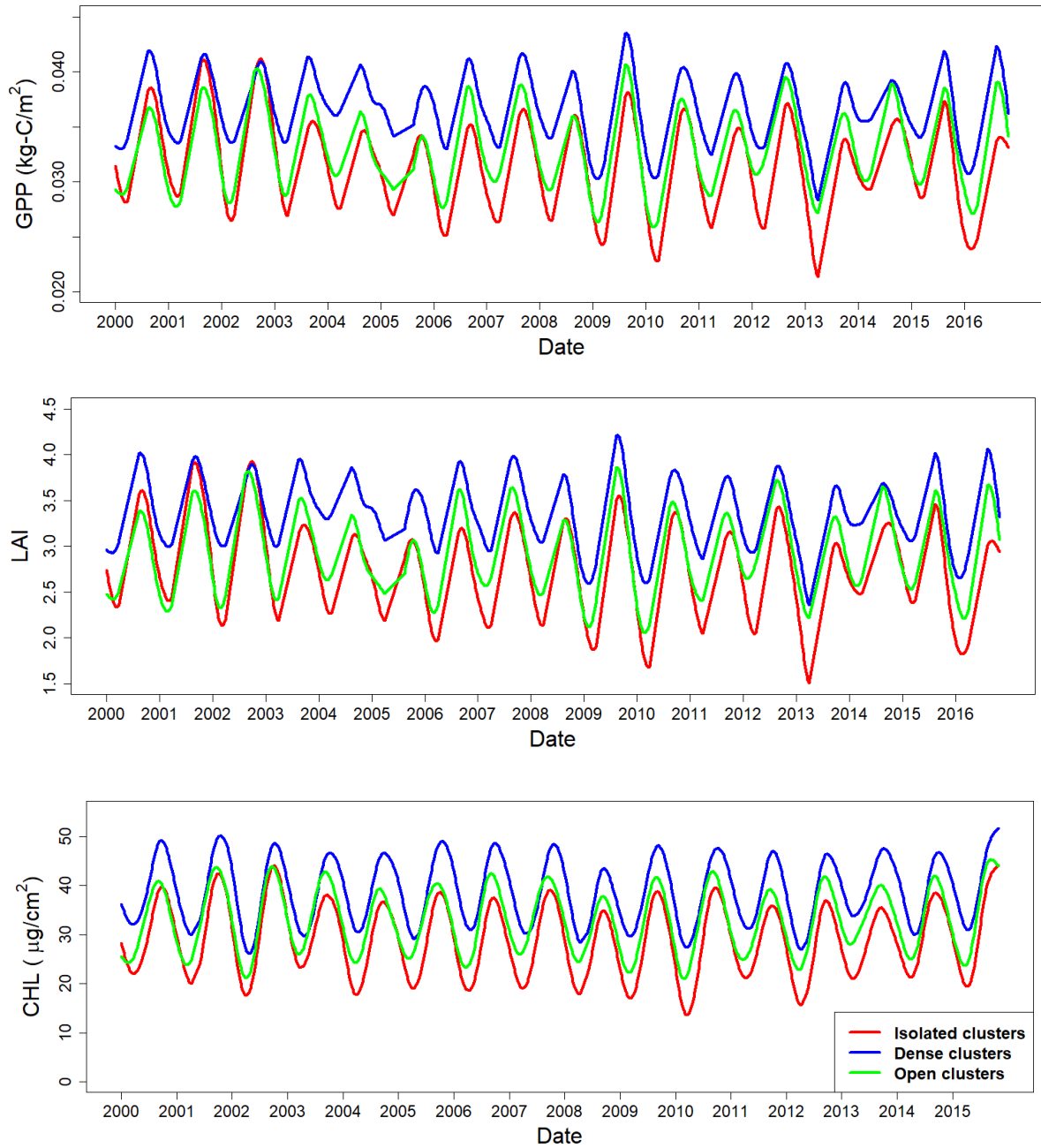


Fig. 9. Long-term (2000-2016) spatio-temporal variability of LAI, CHL, and GPP in isolated, dense and open clusters.

3.2.3 Relationship between Biophysical Parameters and Climatic Variables

Climatic factors such as temperature and precipitation have been found to be closely associated with mangrove biophysical parameters (Kumar et al. 2017). Variability in these climatic factors potentially alters the structure and function of coastal habitats such as mangroves (Rodriguez et al. 2016). Therefore, variability in mangrove biophysical parameters with

physical-meteorological variables including temperature, precipitation, surface runoff and seasonality was analyzed in this study. The final multiple regression model (variables shown in bold in Table 4) revealed that precipitation is positively related to GPP and LAI while negatively related to CHL. The negative relationship of precipitation with CHL could be mainly because of poor photosynthesis during foggy and rainy condition. A previous study by Wei-quing et al. (2015) also found negative impact of precipitation on plant photosynthesis. Further, seasonal variation in rainfall influences chlorophyll content and overall productivity. However, different studies have found different results in relation to effect of precipitation. Flores-de-Santiago et al. (2012) also found different results in concentration of CHL with dry and wet season, that varied with canopy level, species and health of mangrove. It is also because of uneven regional distribution of rainfall. While climate simulations predict increase in rainfall in Central Asia, it is projected to be poor in other parts of South Asia in future (Change 2007). Poor rainfall can affect mangrove productivity, growth and survival by increasing salinity levels. Increase in precipitation results in decrease in salinity, which results in higher productivity and growth. It is also associated with higher run-off, erosion and silt deposition (Upadhyay and Mishra 2010) resulting in accretion of land and associated mangrove migration to newly-built land (Harty 2004, Upadhyay and Mishra 2010).

Our analysis showed that temperature has a negative relationship with all three biophysical parameters. Increase in temperature can disrupt physiological processes including reduction in photosynthetic rates that decrease leaf formation (Saenger and Moverley 1985), that affect the net productivity. High surface temperature also increases evapotranspiration, thus rendering water more saline. IPCC (2007) also stated that increased sea surface temperature has been demonstrated to increase the number and frequency of hurricanes since 1970s. Warming temperature results in ice-melting and oceanic expansion thus triggering sea-level rise that in turn alters mangrove distribution by shifting the species upwards inland. Furthermore, changes in species composition and flowering and fruiting periods (Ellison 2000) are the other responses to increased temperature. In contrast to this study, Rodriguez et al. (2016) found a positive relation between areal extent and seasonal temperature while a negative relation with precipitation in their study on spatio-temporal changes of mangroves in Florida. These variations in the responses to both temperature and precipitation by different studies could be due to a mixture of climatic and ecological processes that operate at multiple scales. The unexplained variation in the biophysical parameters in our models can hence be attributed to other drivers of change not included in the present study, such as frequency of storm events/ disturbances, water quality (salinity, PH, nutrients load etc.), water level, changes in irradiance etc. that control mangrove productivity. However, best combinations of available parameters derived from multiple regression analysis (highlighted in bold in Table 4) were finally utilized in forecasting GPP, LAI, and CHL.

Table 4

Correlation coefficients and percentage of variability explained by individual as well as different combination of physical-meteorological variables in predicting mangrove biophysical parameters (GPP, LAI, CHL).

Meteorological & Physical Variables	(R ²) GPP	Correlation Coefficients (GPP)	(R ²) LAI	Correlation Coefficients	(R ²) CHL	Correlation Coefficients (CHL)
-------------------------------------	--------------------------	-----------------------------------	--------------------------	--------------------------	--------------------------	-----------------------------------

(LAI)						
Temperature	0.35	- (negative)	0.35	- (negative)	0.59	- (negative)
Temperature (1-month lag)	N/A	N/A	N/A	N/A	0.19	- (negative)
Runoff (1-month lag)	0.24	+(positive)	0.24	+(positive)	0.19	+(positive)
Precipitation (1-month lag)	0.25	+(positive)	0.25	+(positive)	0.18	+(positive)
Temperature & Precipitation (1-month lag)	0.54	- (Temp), + (Prec.)	0.54	- (Temp), + (Prec.)	0.71	- (Temp), + (Prec.)
Temperature, Precipitation, Months	0.73	- (Temp), + (Prec.)	N/A	N/A	0.85	- (Temp), - (Prec.)
Temperature, Runoff, Months	N/A	N/A	0.73	- (Temp), - (Runoff)	N/A	N/A
Precipitation, Months	0.69	-(Prec.)	N/A	N/A	N/A	N/A

3.2.4 Forecasting Biophysical Parameters

Visual comparative analysis between current (2016) and forecasted (2050) mean annual GPP, LAI and CHL maps revealed that there was reduction in the values for all three parameters (Figures 10). The mean annual GPP forecasted for 2050 was 7.7% less compared to the mean annual GPP for 2016. The reduction in LAI for year 2050 was 20.83 % compared to mean annual LAI of year 2016. Similarly, the mean annual chlorophyll for year 2050 was forecasted to be 32.9% less compared to the mean annual chlorophyll of year 2016. Analyzing the change in climate between current and projected (2050) years, it was found that the mean annual temperature for year 2016 was 26.6°C, which was projected to increase by 5.03°C in 2050 reaching up to 31.63°C. Similarly, mean annual precipitation for year 2050 was projected to be 150.88 mm, which was 29.88 mm higher compared to the 2016 case.

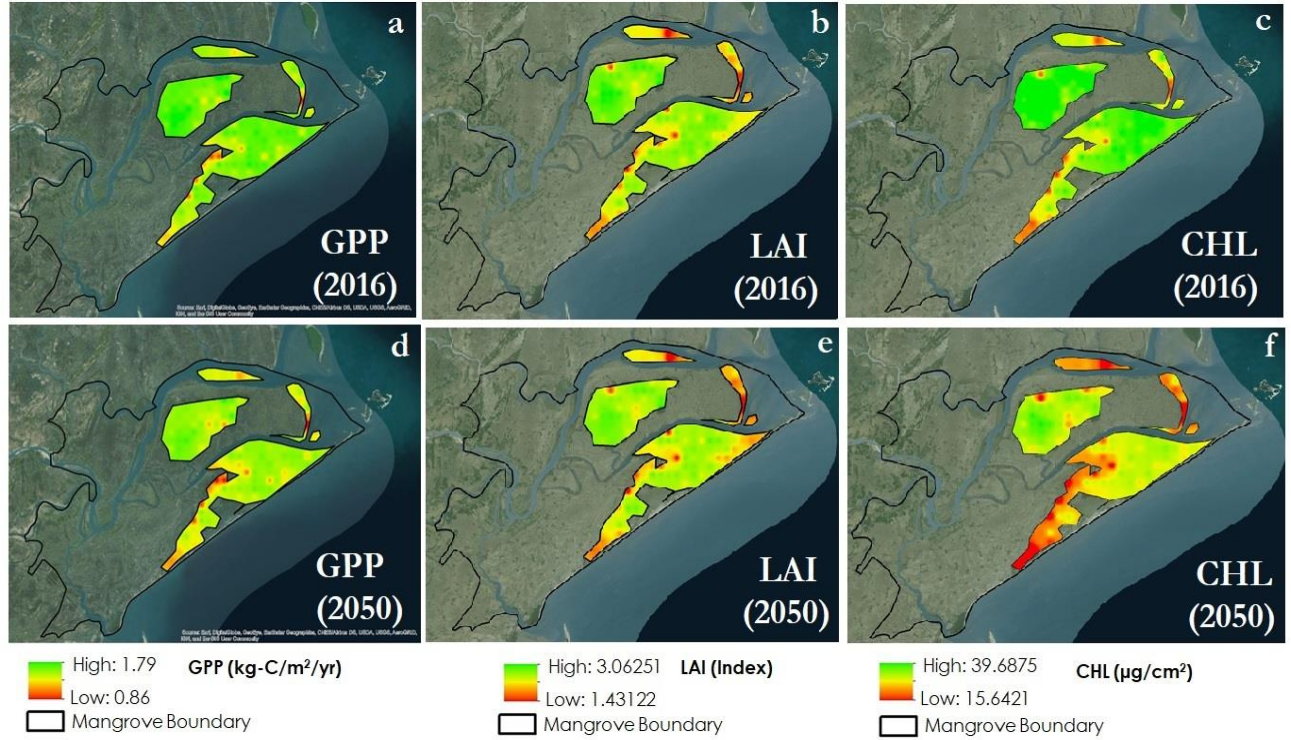


Fig. 9. Comparison between current (2016) and forecasted (2050) mean annual biophysical parameters (GPP, LAI, CHL). MODIS derived GPP, LAI, and CHL data from 2016 were used as a reference for creating current GPP, LAI and CHL maps (a, b, c). The forecasted map

The reduction in CHL between two years was highest compared to the other two parameters. This could potentially be explained based on the coefficients of the meteorological parameters obtained while fitting regression models predicting CHL. Multiple-regression for GPP revealed that it is negatively associated to temperature but positively related to precipitation. In LAI prediction model also, LAI showed negative relation with temperature and positive relationship with precipitation. But in case of CHL prediction model, temperature and precipitation are both negatively related to CHL. Since temperature and precipitation both are projected to increase in future, the reduction in CHL was higher compared to reduction in other parameters. The influence of temperature was relatively higher compared to that of precipitation. Analyzing the spatial variation, the southernmost areas, the isolated areas and some pixels in the boundary have relatively lower values of the biophysical parameters. This could potentially be due to fragmentation and degradation of mangroves.

3.3 Comparison between Forecasted Risk Map and Forecasted Biophysical Parameters

The results from forecasted land cover risk map were in line with the forecasted biophysical parameters map. The assessment of the distributions of mangroves in the past and present and the resulting transition was used to forecast how they will appear in future. Since the dynamics of land cover influence overall productivity of the area, the forecasted biophysical parameters were mapped which identified congruence in the results. Risk map identified lower risk locations around the north-western part of Bhitarkanika that was dominated with dense mangroves, while higher risk areas were identified all along the edges and particularly more

along the isolated clusters and the open mangrove clusters. Forecasted GPP and LAI was found to be lowest along the isolated clusters and open mangroves. Chlorophyll forecast identified mostly the southernmost mangrove patches to be area with lowest chlorophyll content. Dense mangrove patches had relatively high values of all three biophysical parameters. A comparison is shown in Figure 11. Even a single percentage of loss in these biophysical parameters reciprocates into enormous loss in varied ecological services that the mangroves generate. If current trend of degradation continues, not only the carbon stored in mangroves but the future accumulation of carbon could decline. That indicates a grave potential outcome because of the inability to manage mangroves sustainably in the face of climatic changes.

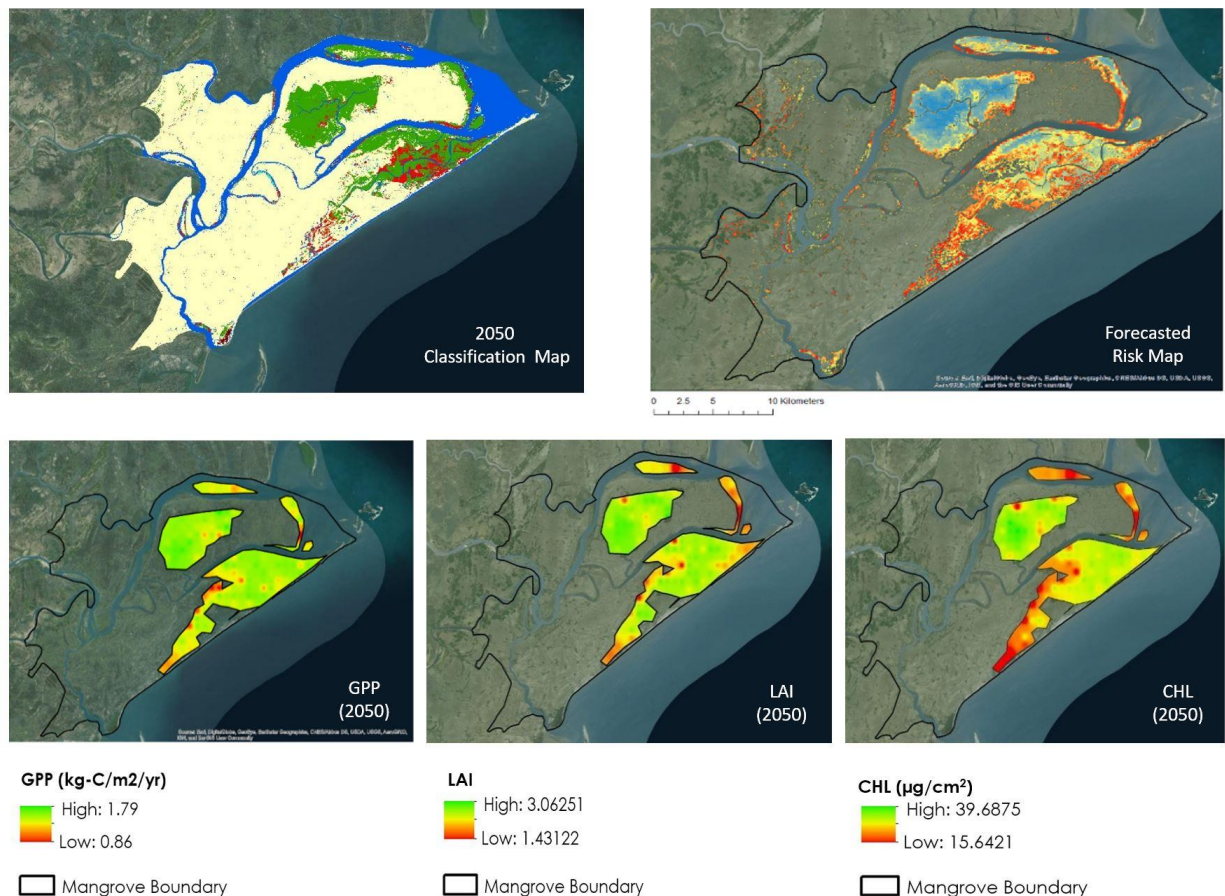


Fig. 10. A comparison between forecasted risk map and forecasted biophysical parameters.

4. Conclusions

This study represents a first attempt to not only quantitatively assess the mangrove extent, spatial distribution pattern and analyze temporal variation, but also to forecast the likely extent and health of Bhitarkanika mangroves in the future, using different biophysical parameters as indicators of mangrove health. The historical analysis of land cover maps using Landsat 5 and 8 data revealed a decrease in dense mangrove extent with an increase in open mangroves and

agricultural area. In addition, forecasted trend suggested decrease in the current extent of dense mangrove up to 10% by the year 2050 despite the conservation efforts. Furthermore, the predicted biophysical parameters as a function of different environmental drivers of change such as temperature and precipitation revealed that GPP and LAI are negatively correlated with surface temperature and positively correlated with precipitation. On the other hand, CHL was found to be negatively correlated with both temperature and precipitation. Forecasted trend of biophysical parameters suggested decrease in annual average GPP, LAI and CHL by 7.7%, 20.83% and 25.96% respectively.

Although the forecasted biophysical maps depict a reasonable spatial and temporal pattern, there is uncertainty associated with them as they were developed under some limitations. The main limitation is that the forecasting model uses only two climatic variables: temperature and precipitation. There are other factors that have been documented to affect mangrove biophysical parameters, such as sea-level rise, salinity, changes in atmospheric CO₂, surface runoff, canopy level, vegetation condition etc. However, limited data availability from a data-scarce region such as the study site restricted the modelling activities. However, a preliminary forecasting model using only temperature and precipitation, the most important drivers could still be revealing the overall trend of the mangrove ecosystem. A future study with more in situ and modeled parameters will be conducted to cross-examine the current forecast model. The correspondence between forecasted risk map and forecasted biophysical parameters indicate overall reliability of the forecast model. Another limitation of the study is the lack of high resolution imagery for land cover classification and lack of in-situ data availability in the study area for model validations.

The degradation of biophysical characteristics, which are also the indicators of mangrove health, vitality and stress, reveals that the mangrove ecosystem of Bhitarkanika wildlife sanctuary may not be able to meet the environmental, economic, and social needs in future. Even a small change in these parameters can cause a huge change in the amount of annual carbon stored by mangroves, thus affecting the regional carbon budget. It is recommended that management efforts focus more on monitoring and restoration programs and policies be implemented to halt immediate conversion of mangroves to other land usage. The study presents a unique combination of multi-sensor based land cover classification and forecasting of mangrove biophysical factors that can be replicated for other coastal mangrove ecosystems being impacted by anthropogenic and climate change, thus leading towards a sustainable management of mangroves globally. It is recommended that future research should include other potential variables including natural and anthropogenic disturbances that can affect the biophysical parameters to be able to better predict future mangrove health.

Acknowledgements

The authors would like to thank the NASA DEVELOP National Program and the Geography Department at University of Georgia for funding and supporting this project. We thank NASA DEVELOP team members at University of Georgia- María José Rivera Araya, Roger Bledsoe, Christopher Cameron, Jessica Staley, Austin Stone and Patricia Stupp for their past contributions to the project. We would like to thank NASA DEVELOP Lead Science Advisor, Dr. Marguerite Madden, at the University of Georgia for providing insight and expertise throughout the project.

We would also like to acknowledge scientists at the Government of Odisha's Chilika Development Authority, especially Dr. Gurdeep Rastogi for their involvement with this work. We would also like to express our gratitude to Dr. Kenton Ross, National Science Advisor from the NASA DEVELOP National Program Office for editing and helping us improve this manuscript. This material is based upon work supported by NASA through contract NNL16AA05C and cooperative agreement NNX14AB60A.

Reference

1. Alongi, D.M., 2002. Present state and future of the world's mangrove forests. *Environmental Conservation*. 29 (03), 331–349.
2. Behera, D.P. and Nayak, L., 2013. Floral Diversity of Bhitarkanika, East Coast of India and its potential uses. *Journal of Chemical, Biological and Physical Sciences (JCBPS)*. 3 (3), 1863.
3. Bhar, S., Chakraborty, D., Ram, S., Das, D., Chakraborty, A., Sudarshan, M. and Santra, S., 2013. Spatial variation of chlorophyll integrity in a mangrove plant (*Excoecaria agallocha*) of Indian Sundarban, with special reference to leaf element and water salinity.
4. Blasco, F., Aizpuru, M. and Gers, C., 2001. Depletion of the mangroves of Continental Asia. *Wetlands Ecology and Management*. 9 (3), 255-266.
5. Change, I.P.O.C., 2007. Climate change 2007: The physical science basis. *Agenda*. 6 (07), 333.
6. Chauhan, R. and Ramanathan, A., 2008. Evaluation of water quality of Bhitarkanika mangrove system, Orissa, east coast of India.
7. Chen, B., Xiao, X., Li, X., Pan, L., Doughty, R., Ma, J., Dong, J., Qin, Y., Zhao, B., Wu, Z., Sun, R., Lan, G., Xie, G., Clinton, N. and Giri, C., 2017. A mangrove forest map of China in 2015: Analysis of time series Landsat 7/8 and Sentinel-1A imagery in Google Earth Engine cloud computing platform. *ISPRS Journal of Photogrammetry and Remote Sensing*. 131, 104-120.
8. Clarke, P.J., Kerrigan, R.A. and Westphal, C.J., 2001. Dispersal potential and early growth in 14 tropical mangroves: do early life history traits correlate with patterns of adult distribution? *Journal of Ecology*. 89 (4), 648-659.
9. Cougo, M., Souza-Filho, P., Silva, A., Fernandes, M., Santos, J., Abreu, M., Nascimento, W. and Simard, M., 2015. Radarsat-2 Backscattering for the Modeling of Biophysical Parameters of Regenerating Mangrove Forests. *Remote Sensing*. 7 (12), 17097-17112.
10. Das, S. and Vincent, J.R., 2009. Mangroves protected villages and reduced death toll during Indian super cyclone. *Proceedings of the National Academy of Sciences*. 106 (18), 7357-7360.
11. Eastman, J.R., 2015. TerrSet manual. Accessed in TerrSet version. 18, 1-390.
12. Ellison, J.C. 2000 How South Pacific mangroves may respond to predicted climate change and sea-level rise. In *Climate change in the South Pacific: impacts and responses in Australia, New Zealand, and small island states*, Springer, pp. 289-300.
13. Field, C., 1994. Assessment and monitoring of climate change impacts on mangrove ecosystems. *UNEP Regional Seas Reports and Studies*. 154, 62.

14. Flores-de-Santiago, F., Kovacs, J.M. and Flores-Verdugo, F., 2012. Seasonal changes in leaf chlorophyll a content and morphology in a sub-tropical mangrove forest of the Mexican Pacific. *Marine Ecology Progress Series*. 444, 57-68.
15. Giri, C., 2016. Observation and Monitoring of Mangrove Forests Using Remote Sensing: Opportunities and Challenges. *Remote Sensing*. 8 (9), 783.
16. Giri, C., Long, J., Abbas, S., Murali, R.M., Qamer, F.M., Pengra, B. and Thau, D., 2015. Distribution and dynamics of mangrove forests of South Asia. *Journal of environmental management*. 148, 101-111.
17. Giri, C., Ochieng, E., Tieszen, L.L., Zhu, Z., Singh, A., Loveland, T., Masek, J. and Duke, N., 2011. Status and distribution of mangrove forests of the world using earth observation satellite data. *Global Ecology and Biogeography*. 20 (1), 154-159.
18. Giri, C., Pengra, B., Zhu, Z., Singh, A. and Tieszen, L.L., 2007. Monitoring mangrove forest dynamics of the Sundarbans in Bangladesh and India using multi-temporal satellite data from 1973 to 2000. *Estuarine, Coastal and Shelf Science*. 73 (1-2), 91-100.
19. Gislason, P.O., Benediktsson, J.A. and Sveinsson, J.R., 2006. Random forests for land cover classification. *Pattern Recognition Letters*. 27 (4), 294-300.
20. Hamilton, S.E. and Casey, D., 2016. Creation of a high spatio-temporal resolution global database of continuous mangrove forest cover for the 21st century (CGMFC-21). *Global Ecology and Biogeography*. 25 (6), 729-738.
21. Harty, C., 2004. Planning Strategies for Mangrove and Saltmarsh Changes in Southeast Australia. *Coastal Management*. 32 (4), 405-415.
22. Horning, N. Random Forests: An algorithm for image classification and generation of continuous fields data sets.
23. Hussain, S.A. and Badola, R., 2010. Valuing mangrove benefits: contribution of mangrove forests to local livelihoods in Bhitarkanika Conservation Area, East Coast of India. *Wetlands Ecology and Management*. 18 (3), 321-331.
24. Ibharim, N., Mustapha, M.A., Lihan, T. and Mazlan, A., 2015. Mapping mangrove changes in the Matang Mangrove Forest using multi temporal satellite imageries. *Ocean & Coastal Management*. 114, 64-76.
25. Ishtiaque, A., Myint, S.W. and Wang, C., 2016. Examining the ecosystem health and sustainability of the world's largest mangrove forest using multi-temporal MODIS products. *Science of the Total Environment*. 569, 1241-1254.
26. Kamal, M. and Phinn, S., 2011. Hyperspectral data for mangrove species mapping: A comparison of pixel-based and object-based approach. *Remote Sensing*. 3 (10), 2222-2242.
27. Kamal, M., Phinn, S. and Johansen, K., 2015. Object-based approach for multi-scale mangrove composition mapping using multi-resolution image datasets. *Remote Sensing*. 7 (4), 4753-4783.
28. Kandasamy, K. 2017 Mangroves in India and Climate Change: An Overview. In *Participatory Mangrove Management in a Changing Climate*, Springer, pp. 31-57.
29. Kathiresan, K. and Bingham, B.L., 2001. Biology of mangroves and mangrove ecosystems. *Advances in marine biology*. 40, 81-251.
30. Kuenzer, C., Bluemel, A., Gebhardt, S., Quoc, T.V. and Dech, S., 2011. Remote sensing of mangrove ecosystems: A review. *Remote Sensing*. 3 (5), 878-928.

31. Kumar, A., Stupp, P., Dahal, S., Remillard, C., Bledsoe, R., Stone, A., Cameron, C., Rastogi, G., Samal, R. and Mishra, D.R., 2017. A Multi-Sensor Approach for Assessing Mangrove Biophysical Characteristics in Coastal Odisha, India. *Proceedings of the National Academy of Sciences, India Section A: Physical Sciences*. 1-22.
32. Manson, F.J., Loneragan, N.R., Skilleter, G.A. and Phinn, S.R., 2005. An evaluation of the evidence for linkages between mangroves and fisheries: a synthesis of the literature and identification of research directions.
33. Mazda, Y., Magi, M., Kogo, M. and Hong, P.N., 1997. Mangroves as a coastal protection from waves in the Tong King delta, Vietnam. *Mangroves and Salt Marshes*. 1 (2), 127-135.
34. Nagelkerken, I., Blaber, S., Bouillon, S., Green, P., Haywood, M., Kirton, L., Meynecke, J.-O., Pawlik, J., Penrose, H. and Sasekumar, A., 2008. The habitat function of mangroves for terrestrial and marine fauna: a review. *Aquatic Botany*. 89 (2), 155-185.
35. Nemani, R., Votava, P., Michaelis, A., White, M., Melton, F., Coughlan, J., Golden, K., Hashimoto, H., Ichii, K. and Johnson, L., 2007. Terrestrial Observation and Prediction System (TOPS): Developing ecological nowcasts and forecasts by integrating surface, satellite and climate data with simulation models. *Research and Economic Applications of Remote Sensing Data Products*, edited by U. Aswathanarayana and R. Balaii. London: Taylor and Francis.
36. Parida, A., Das, A.B. and Das, P., 2002. NaCl stress causes changes in photosynthetic pigments, proteins, and other metabolic components in the leaves of a true mangrove, *Bruguiera parviflora*, in hydroponic cultures. *Journal of Plant Biology*. 45 (1), 28-36.
37. Pastor-Guzman, J., Atkinson, P.M., Dash, J. and Rioja-Nieto, R., 2015. Spatiotemporal variation in mangrove chlorophyll concentration using Landsat 8. *Remote Sensing*. 7 (11), 14530-14558.
38. Patil, V., Singh, A., Naik, N. and Unnikrishnan, S., 2015. Estimation of mangrove carbon stocks by applying remote sensing and GIS techniques. *Wetlands*. 35 (4), 695-707.
39. Pattanaik, C., Reddy, C.S., Murthy, M. and Swain, D. 2008 Assessment and Monitoring the Coastal Wetland Ecology Using RS and GIS with Reference to Bhitarkanika Mangroves of Orissa, India. In *Monitoring and Modelling Lakes and Coastal Environments*, Springer, pp. 226-236.
40. Reddy, C., Pattanaik, C., Dhal, N. and Biswal, A., 2006. Vegetation and floristic diversity of Bhitarkanika National Park, Orissa, India. *Indian Forester*. 132 (6), 664.
41. Reddy, C.S., Pattanaik, C. and Murthy, M., 2007. Assessment and monitoring of mangroves of Bhitarkanika Wildlife Sanctuary, Orissa, India using remote sensing and GIS. *Current Science*. 1409-1415.
42. Rodríguez Eraso, N., Armenteras-Pascual, D. and Alumbrosos, J.R., 2013. Land use and land cover change in the Colombian Andes: dynamics and future scenarios. *Journal of Land Use Science*. 8 (2), 154-174.
43. Rodriguez, W., Feller, I.C. and Cavanaugh, K.C., 2016. Spatio-temporal changes of a mangrove–saltmarsh ecotone in the northeastern coast of Florida, USA. *Global Ecology and Conservation*. 7, 245-261.
44. Saenger, P. and Moverley, J. Vegetative phenology of mangroves along the Queensland coastline, pp. 257-265.

45. Selvam, V., Ravichandran, K., Gnanappazham, L. and Navamuniyammal, M., 2003. Assessment of community-based restoration of Pichavaram mangrove wetland using remote sensing data. *Current science*. 794-798.
46. Solomon, S., 2007. Climate change 2007-the physical science basis: Working group I contribution to the fourth assessment report of the IPCC. Cambridge University Press.
47. Upadhyay, V. and Mishra, P., 2010. Phenology of mangroves tree species on Orissa coast, India. *Tropical Ecology*. 51 (2), 289.
48. Ward, R.D., Friess, D.A., Day, R.H. and MacKenzie, R.A., 2016. Impacts of climate change on mangrove ecosystems: a region by region overview. *Ecosystem Health and Sustainability*. 2 (4)
49. Weber, S.J., Keddell, L. and Kemal, M., 2014. Myanmar Ecological Forecasting: Utilizing NASA Earth Observations to Monitor, Map, and Analyze Mangrove Forests in Myanmar for Enhanced Conservation.
50. Wei-qing, Y., Yun-qi, W., Hui-lan, Z., Bin, W. and Yong, L., 2015. Effect of precipitation condition on photosynthesis and biomass accumulation and referring to splash erosion status in five typical evergreen tree species in humid monsoon climatic region of subtropical hill-land. *Journal of Central South University*. 22, 3795-3805.
51. Zebiak, S.E., 2003. Research potential for improvements in climate prediction. *Bulletin of the American Meteorological Society*. 84 (12), 1692-1696.